

1 **"Phylogenetic analysis of *ABCE* genes across the plant kingdom"**

2 **Liina Jakobson^{1,2*±}, Jelena Mõttus^{1,*±}, Jaanus Suurväli³, Merike Sõmera¹, Jemilia Tarassova¹,**

3 **Lenne Nigul¹, Olli-Pekka Smolander¹, Cecilia Sarmiento^{1,*}**

4 ¹ Department of Chemistry and Biotechnology, Tallinn University of Technology, Akadeemia tee 15,
5 12618 Tallinn, Estonia.

6 ² Current affiliation: Plant Biotechnology Department, Centre of Estonian Rural Research and Knowledge,
7 M. Pilli haru 1, 48309 Jõgeva, Estonia.

8 ³ Department of Biological Sciences, University of Manitoba, 50 Sifton Rd, Winnipeg, MB, R3T 2N2,
9 Canada.

10 **± Equal contribution**

11 * Authors for Correspondence: Liina Jakobson, Plant Biotechnology Department, Centre of Estonian Rural
12 Research and Knowledge, M. Pilli haru 1, Jõgeva, Estonia, +372 5199 5445, liina.jakobson@metk.agri.ee;
13 Cecilia Sarmiento, Department of Chemistry and Biotechnology, Tallinn University of Technology,
14 Akadeemia tee 15, 12618, Estonia, +372 56285691, cecilia.sarmiento@taltech.ee

16 **Abstract**

17 ATP-BINDING CASSETTE SUBFAMILY E MEMBER (*ABCE*) proteins are one of the most conserved
18 proteins across eukaryotes and archaea. Yeast and the vast majority of animals possess a single *ABCE* gene
19 encoding the vital *ABCE1* protein. We retrieved *ABCE* gene sequences of 76 plant species from public
20 genome databases and analyzed them with the reference to *Arabidopsis thaliana ABCE2* gene (*AtABCE2*).
21 Over half of the studied plant species possess two or more *ABCE* genes. There can be as many as eight
22 *ABCE* genes in a plant species. This suggest that *ABCE* genes in plants can be classified as a low-copy gene
23 family, rather than a single-copy gene family. Plant *ABCE* proteins showed overall high sequence
24 conservation, sharing at least 78% of amino acid sequence identity with *AtABCE2*. The phylogenetic trees
25 of full-length *ABCE* amino acid and CDS sequences demonstrated that *Brassicaceae* and *Poaceae* families

26 have independently undergone lineage-specific split of the ancestral *ABCE* gene. Other plant species have
27 gained *ABCE* gene copies through more recent duplication events. Deeper analysis of *AtABCE2* and its
28 paralogue *AtABCE1* from 1135 *Arabidopsis thaliana* ecotypes revealed 4 and 35 non-synonymous SNPs,
29 respectively. The lower natural variation in *AtABCE2* compared to *AtABCE1* is in consistence with its
30 crucial role for plant viability. Overall, while the sequence of the ABCE protein family is highly conserved
31 in the plant kingdom, many plants have evolved to have more than one copy of this essential translational
32 factor.

33

34 **Key words:** *ABCE* gene subfamily, ABCE, gene evolution, phylogenetics, natural variation, plants

35 **Significance statement:**

36 In most eukaryotes there is a single ABCE protein, which is involved in many vital processes in cells.
37 However, less is known about ABCEs specifically in plants. Here we show that while the sequence of ABCE
38 proteins is highly conserved in plants, they have evolved to often have multiple copies of this essential
39 translational factor. By studying 76 species from the entire plant kingdom, we observed as many as eight
40 *ABCE* genes being present at a time, although most species have less. Some *ABCE* copies appeared earlier
41 than others and were found in multiple species. Thus, our findings indicate that ABCE genes in plants are
42 not a single-copy gene family and should instead be re-classified as a low-copy gene family.

43

44 **Data Availability Statement:**

45 Multiple sequence alignments of plant ABCE protein sequences used in this study have been made publicly
46 available at Dryad repository (Jakobson, Liina (2022), Plant ABCEs, Dryad, Dataset,
47 <https://doi.org/10.5061/dryad.vhhmgqz2>).

48 **Introduction**

49 Members of the ATP-BINDING CASSETTE (ABC) subfamily E (ABCE) belong to the
50 superfamily of ABC proteins, which can be found in all living organisms studied to date and are regarded
51 as highly essential in all eukaryotes. Most ABC proteins function as ATP-dependent membrane transporters.
52 They possess transmembrane domains (TMDs) coupled with nucleotide-binding domains (NBD) otherwise
53 known as ATP-binding cassettes (Andolfo et al. 2015; Navarro-Quiles et al. 2018). ABCE (initially denoted
54 RNASE L INHIBITOR (RLI)) proteins, in contrast, lack TMDs, but still have two NBDs associated with
55 several specific domains and thus are soluble proteins.

56 In most species the ABCE subfamily is represented by a single member, ABCE1, which is involved
57 in ribosome biogenesis and several stages of translation regulation (Yarunin et al. 2005; Andersen & Leever
58 2007; Barthelme et al. 2011; Mancera-Martínez et al. 2017; Navarro-Quiles et al. 2018). In accordance with
59 its fundamental role, ABCE1 expression has been detected in most tissues and developmental stages of the
60 species studied. In addition, loss-of-function of *ABCE1* genes results in a lethal phenotype in all studied
61 species (Du et al. 2003; Zhao et al. 2004; Maeda et al. 2005; Sarmiento et al. 2006; Kougioumoutzi et al.
62 2013). ABCE1 has been found to participate in translational initiation and termination, however, its most
63 conserved function is in the process linking these two stages of translation – ribosome recycling (Navarro-
64 Quiles et al. 2018). During that process, ABCE1 splits the ribosome through direct interactions with
65 ribosomal subunits and release factors, either after canonical stop codon-dependent termination or after
66 recognition of stalled and vacant ribosomes. The latter is recognized during mRNA surveillance
67 mechanisms such as no-go decay (NGD), non-stop decay (NSD), and non-functional 18S rRNA decay (18S-
68 NRD) (Graille & Séraphin 2012). Furthermore, ABCE1 dissociates the 80S-like complex during maturation
69 of ribosomal subunits (Strunk et al. 2012). The role in ribosome biogenesis is supported by the nuclear
70 accumulation of 40S and 60S ribosome subunits in the absence of ABCE1 (Yarunin et al. 2005; Kispal et
71 al. 2005; Andersen & Leever 2007). Additionally, it has a key role in RNA silencing in both plants and
72 animals (Zimmerman et al. 2002; Sarmiento et al. 2006; Kärblane et al. 2015). Moreover, we have

73 previously shown that human ABCE1 (HsABCE1) is directly or indirectly involved in histone biosynthesis
74 and DNA replication (Toompuu et al. 2016).

75 The study of ABCE functions in plants has been mostly limited to the model plants *Arabidopsis*
76 *thaliana*, *Nicotiana benthamiana*, *Nicotiana tabacum* and *Cardamine hirsuta* (Petersen et al. 2004;
77 Sarmiento et al. 2006; Kougioumoutzi et al. 2013; Möttus et al. 2021; Navarro-Quiles et al. 2022). In *A.*
78 *thaliana* there are two genes encoding for paralogous ABCE proteins (AtABCE1 and AtABCE2, also
79 referred to as AtRLI1 and AtRLI2, respectively), which share 80.8% identity (Navarro-Quiles et al. 2022;
80 Möttus et al. 2021). AtABCE2 is orthologous to HsABCE1 and is ubiquitously expressed in all plant organs
81 (Sarmiento et al. 2006). Recently, AtABCE2 was found to interact with ribosomal proteins and translational
82 factors, confirming its conserved ancestral function in translation that is coupled to general growth and
83 vascular development, likely indirectly via auxin metabolism (Navarro-Quiles et al. 2022). Furthermore,
84 through regulation of translation AtABCE2 is involved in the development of gametophyte and embryo
85 (Yu, et al. 2023). In addition, AtABCE2 has been shown to suppress GFP transgene RNA silencing in
86 heterologous system at the local and at the systemic levels by reducing accumulation of siRNAs (Sarmiento
87 et al. 2006; Kärblane et al. 2015). Mutational analysis of AtABCE2 revealed that the structural requirements
88 for RNA silencing suppression are similar to those needed for ribosome recycling in archaea (Möttus et al.
89 2021). This indicates that AtABCE2 might suppress RNA silencing via supporting translation-associated
90 RNA degradation mechanisms. The role of AtABCE1 in *A. thaliana*, which is expressed almost exclusively
91 in generative organs (Navarro-Quiles et al 2022; Yu et al 2023), is yet to be studied.

92 Silencing of *ABCE* orthologues (*RLIh*) in *N. tabacum* resulted in a single viable transgenic plant
93 exhibiting severe morphological alterations, supporting the important role of ABCE proteins at the whole-
94 organism level. At that time, it remained unclear how many *RLIh* genes there are in tobacco species
95 (Petersen et al. 2004). In *C. hirsuta*, a close relative of *A. thaliana* that has composite leaves, there is only
96 one *ABCE* gene in the genome, named SIMPLE LEAF3 (SIL3, or ChRLI2) (Kougioumoutzi et al. 2013).
97 Hypomorphic mutation Pro177Leu in the NBD1 domain of ChRLI2 affects the determination of leaf shape
98 and regulation of auxin homeostasis (Kougioumoutzi et al. 2013). Interestingly, the expression of *ChRLI2*

99 was not ubiquitous as in *A. thaliana*, but instead it was shown to be expressed in meristematic and vascular
100 tissues of young developing leaves and in leaflet initiation sites (Kougioumoutzi et al. 2013).

101 It is commonly claimed that most eukaryotes only have one *ABCE* gene (Dermauw & Van Leeuwen
102 2014). Exceptions to this have been detected in plants such as thale cress, rice, maize, potato and tomato,
103 but also in animals such as catfish, cod and mosquitoes (Braz et al. 2004; Garcia et al. 2004; Verrier et al.
104 2008; Liu et al. 2013; Pang et al. 2013; Andolfo et al. 2015; Lu et al. 2016). Although some plant species
105 have more than one *ABCE* gene, it is still the smallest and most conserved of all ABC subfamilies (Andolfo
106 et al. 2015).

107 In this study we aimed to characterize the phylogenetic evolution of *ABCE* genes in plants in order
108 to shed light on the possible functional diversification within ABCE protein family. Here we present the
109 results of an extensive bioinformatics analysis of publicly available sequences for plant *ABCE* genes and
110 corresponding proteins, together with haplotype analysis of *A. thaliana* *ABCE*s.

111

112 **Results**

113 **Variability of plant *ABCE* genes**

114 To gain insight into the diversity of *ABCE* genes in plants, we compiled a selection of *ABCE* genes
115 from 76 different plant species available in public databases. The selection criteria for including in further
116 analysis was high identity (min 78%) of the full-length amino acid sequence to AtABCE2 and the presence
117 of all known essential structural elements of ABCE proteins (Karcher et al. 2005; Barthelme et al. 2007;
118 Nürenberg & Tampé 2013; Nürenberg-Goloub et al. 2020). Truncated or aberrant sequences were discarded
119 from further analysis. Altogether 152 plant *ABCE* genes were included in the study. The selected species
120 represented a wide range of plant groups, including unicellular algae such as *Chlamydomonas reinhardtii*
121 and *Micromonas sp. RCC299*, monocots such as *Zea mays* and *Triticum aestivum*, *Solanum* species such as
122 *Solanum tuberosum* and *N. benthamiana*, and *Brassicaceae* such as *Brassica napus* and *A. thaliana* (Figure
123 1, Supplementary Table S1). Our analysis revealed that plant species from the phylum *Chlorophyta* (green

124 algae) usually possess only a single *ABCE* gene, except for *Ostreococcus lucimarinus*, which has two genes.
125 In contrast, most of the analyzed species in the *Poaceae* family have at least two *ABCE* genes, and some
126 have as many as eight genes in their genome, as is the case for *T. aestivum*. Another group of plant species
127 with an above-average number of *ABCE* genes is the *Brassicaceae* family. For example, *B. napus* has eight
128 genes, *B. rapa* five genes, and *Capsella rubella* four genes. On the other hand, among *Brassicaceae*, *C.*
129 *hirsuta* and *Boechera stricta* have only a single *ABCE* gene (Figure 1). Interestingly, only 30 species out of
130 76 (39.5%) had a single *ABCE* gene. Similarly, there were 34 species (44.7%) possessing two *ABCE* genes
131 (Figure 2A). This shows that *ABCE* genes in plants are not a single-copy gene family and should instead be
132 re-classified as a low-copy gene family.

133 Next, we analyzed the correlation between ploidy level and the number of *ABCE* genes. Despite
134 clustering of multi-gene-species in the *Poaceae* and *Brassicaceae* families, there was no visual segmentation
135 between the number of *ABCE* genes and phylogenetic origin in other plant families (Figure 1). We found a
136 slight correlation ($R=0.25$) between ploidy level and the amount of *ABCE* genes per species. However, there
137 were examples of tetraploid species with a single *ABCE* gene (e.g. *S. tuberosum*) and diploids with five
138 *ABCE* genes (e.g. *B. distachyon*, *B. rapa*) (Figure 2B, Supplementary Table S1).

139 We compared the amount of *ABCE* genes with known whole genome duplications (WGDs) and
140 triplications (WGT) per species. WGD data was based on the data of 53 plant species published by the One
141 Thousand Plant Transcriptomes Initiative (Leebens-Mack et al. 2019). The observation of WGT data in the
142 common ancestor of *Brassica* species was based on the study of Wang and coworkers (Wang et al. 2011).
143 We found a very weak correlation ($R=0.17$) between the number of *ABCE* genes in a species and the number
144 of WGD events that have taken place in the ancestors of the respective species (Figure 2C). Interestingly,
145 there are examples of species, which have encountered at least five WGDs in their evolutionary history, but
146 still possess only a single *ABCE* gene, for example *Actinidia chinensis* and *Glycine max* (Figure 1, 2C,
147 Supplementary Table S2).

148 **Plant *ABCE*s are highly conserved**

149 ABCE proteins are composed of four domains: NBD1 and NBD2 forming the ATPase core,
150 bipartite hinge domain that is tightly engaged in twin-NBD cassette arrangement and a unique N-terminal
151 iron-sulphur (FeS) cluster domain (Figure 3A). Additionally, ABCEs embody a helix–loop–helix (HLH)
152 motif in NBD1 that distinguishes it from otherwise superimposable NBD2 (Karcher et al. 2005).

153 As many as 86.8% out of the 152 analyzed gene sequences encode ABCE of canonical protein
154 length (600–609 amino acids) (Figure 3B). Along with exceptional conservation within functionally critical
155 motifs, all analyzed ABCE sequences are highly similar to AtABCE2 sharing at least 78% of amino acid
156 sequence identity (Figure 3C, Supplementary Table S3).

157 We also plotted amino acid sequence length to amino acid sequence identity for the studied 152
158 ABCE proteins. There was a clear clustering of proteins with the length of 605 amino acids (Figure 3D).
159 Proteins with lower sequence identity did not cluster by protein length (Figure 3D). Interestingly, proteins
160 with more than 90% identity to AtABCE2 could be as short as 591 amino acids and as long as 625 amino
161 acids long (Figure 3D). Hence, despite some variance in amino acid sequence length and sequence identity
162 to AtABCE2, the selection of amino acid sequences analyzed here is uniform and represents well the plant
163 *ABCE* genes.

164 **Phylogeny of plant *ABCE*s**

165 To understand how ABCE proteins have evolved in the green plant lineage, we constructed a
166 Maximum Likelihood (ML) phylogenetic tree for 152 ABCE protein sequences from 76 species (Figure 4).
167 Among the included species, *Chlorophyta* (green algae) represent the earliest lineage to split off from the
168 rest of the green plants. In an unrooted tree of ABCE amino acid sequences, representatives of *Chlorophyta*
169 formed a separate cluster with high bootstrap support (Supplementary Figure S1a). In a smaller tree with
170 ABCE amino acid sequences from 15 plant species rooted with HsABCE1, the sequences from *Chlorophyta*
171 were clearly split off from all other plants (Supplementary Figure S1b). We therefore reasoned that
172 *Chlorophyta* would be a suitable outgroup for rooting the tree.

173 By examining the tree rooted on *Chlorophyta*, we found that most of the plant ABCE full-length
174 protein sequences cluster well together according to the taxonomic groupings. For instance, ABCEs from
175 *Fabaceae* family members (legumes) form a single cluster, as is the case for *Solanaceae* family
176 (nightshades). Homologous ABCE protein sequences from these families share a very high similarity and
177 likely have the same function (Figure 4). As previously reported for a small selection of *Brassicaceae*
178 (mustard and cabbage family, includes the thale cress *A. thaliana*) (Navarro-Quiles et al. 2022), our analysis
179 shows that many of their members encode distinguishable ABCE1 and ABCE2 proteins (Figure 4). Notably,
180 all *Brassicaceae* species have at least one ABCE2 protein.

181 In contrast to the well supported clustering of sequences from the same taxonomic groups,
182 relationships between the clusters were not fully resolved and all internal branches of the tree were poorly
183 supported. The topology of the likeliest amino acid sequence-based tree suggested all ABCE proteins from
184 *Poaceae* (grasses) to be more closely related to AtABCE1 than to AtABCE2. This contrasts the notion that
185 AtABCE2 preserves the ancestral function, whereas AtABCE1 is subjected to ongoing subfunctionalization
186 or pseudogenization (Navarro-Quiles et al. 2022). In an attempt to shed further light on the phylogenetic
187 relationships between AtABCE proteins and ABCEs from *Poaceae* family members, we constructed an
188 additional tree including ABCE amino acid sequences from the *Brassicaceae* (32) and *Poaceae* (48)
189 families, together with *Amborella trichopoda* (2), an important reference plant species in evolutionary
190 studies. The green algae *C. reinhardtii* (1) was used to root the tree. In the likeliest tree obtained from this
191 analysis, *Brassicaceae* ABCE1 group appeared as a separate branch, whereas all *Poaceae* ABCE protein
192 sequences clustered together with AtABCE2, a very different result than the one obtained before. This
193 further highlights that the amino acid sequences of ABCE may not be sufficient to fully resolve the
194 phylogeny (Figure 5).

195 We then constructed an additional ML-tree based on nucleotide sequences coding for the ABCE
196 proteins (coding sequence; CDS), rather than the proteins themselves. We used CDS of the same 152 plant
197 ABCE proteins that were used to generate Figure 4, and again used *Chlorophyta* as an outgroup for placing
198 the root (Figure 6). The information provided by nucleotide-level differences allowed additional branches

199 in the tree to be resolved with high bootstrap support values. Here it becomes clear that the split of a single
200 *ABCE* gene into *ABCE1* and *ABCE2* happened in the common ancestor of *Brassicaceae*, whereas the
201 ancestor of *Poaceae* had a similar split independently (Figure 6). Furthermore, it appears that in the common
202 ancestor of the largest *Poaceae* subfamily *Pooideae*, involving important cereals such as barley and wheat,
203 one *ABCE* paralogue went through additional duplication (Figure 6). Although many other plant species
204 also have more than one *ABCE* gene, these originate from more recent duplication events that are usually
205 not shared with other analyzed species. The placement of major clusters in relation to each other generally
206 correlates with the species tree (Figure 6).

207 In addition, we separately analyzed the three main domains of ABCE proteins, FeS cluster domain,
208 NBD1, and NBD2, by realigning the corresponding sequences and constructing a ML-tree for each
209 (Supplementary Figure S2, S3, S4). The topology of the resulting trees was different for each domain, but
210 none of those were well supported by bootstrap analysis.

211 **Natural variation of Arabidopsis *AtABCE1* and *AtABCE2* genes**

212 Natural variation among *A. thaliana* ecotypes has been well documented by the 1001 Genomes
213 Project (Weigel & Mott 2009). We analyzed the *ABCE* gene sequences of all 1135 *A. thaliana* ecotypes
214 reported in that project and found 35 and 4 non-synonymous SNPs in *AtABCE1* and *AtABCE2*, respectively
215 (Supplementary Table S4). Only four non-synonymous SNPs in *AtABCE2* indicate a low degree of natural
216 variation, which is consistent with its fundamental, conserved role in growth and development. On the other
217 hand, 35 non-synonymous SNPs annotated for *AtABCE1* show relatively higher natural variation. From
218 these SNPs, we selected 18 that cause amino acid substitutions at conserved and important positions or that
219 were present in combination with other SNPs of interest. Therefore, 21 ecotypes were included in the further
220 study and resequencing, together with Col-0 (Supplementary Table S4; Table 1). Two SNPs causing amino
221 acid substitution could not be detected while resequencing (Pro399Thr in Grivo-1 and Gly182Ser in IP-Cot-
222 0). Instead, one SNP previously undocumented in the 1001 Genomes Project database (Leu253Phe in Grivo-
223 1) was identified. Figure 7A shows the positions of the amino acid substitutions caused by the 17 SNPs

224 sequenced in the *AtABCE1* gene. In our resequencing analysis, the most frequent SNPs in *AtABCE1* caused
225 the changes His561Leu and Ala441Thr (Table 1). Noteworthy, histidine at the position 561 seems to be
226 characteristic to Col-0, as all the other analyzed ecotypes had leucine at this position. Next, we performed
227 haplotype analysis with CDS sequences on the PopART platform and found that the most conserved
228 sequence of *AtABCE1* is most probably the one identical to Ei-2, Kia1, Pra-6, IP-Car-1 and Can-0 (Figure
229 7B). Eight SNPs out of 17 appear as single SNPs in the *AtABCE1* of Kly4, Toufl-1, Col-0, IP-Ezc-2, IP-
230 Vis-0, IP-Moz-0, IP-Hoy-0, IP-Loz-0, IP-Cot-0 and Lebja-1 (Figure 7B). Interestingly, a substitution of
231 Ala441Thr can appear both as the consequence of a single SNP in Leska-1-44 and together with other SNPs
232 such as in Cvi-0 or Qar-8a (Figure 7B). Some amino acid changes, like Pro129Gln, Ala549Gly and
233 His561Leu, are always grouped (Table 1). Pro129Gln appears only together with at least two other SNPs,
234 e.g., in Grivo-1 or Qar-8a (Figure 7B).

235 In *AtABCE2*, we found only three amino acid changes (Gly44Ser, Met379Thr and Gly405Ala) due
236 to non-synonymous SNPs, which were located in FeS cluster domain and NBD2 at not conserved positions
237 (Figure 7C; Supplementary Table S4). The SNPs were verified in five different ecotypes (Table 1). The
238 haplotype map of *AtABCE2* SNPs shows that Col-0 has the most conserved sequence and three different
239 SNPs root from it (Figure 7D).

240 In this study we could not find any correlation between the presence of non-synonymous SNPs in
241 *AtABCE* genes and the geographical origin of the ecotype (Table 1). Visual rosette phenotype of the studied
242 ecotypes matched with characterization available in the public databases (Supplementary Figure S5).

243 In the case of 18 out of 21 ecotypes, all SNPs were confirmed as reported earlier. For three ecotypes
244 only part of the SNPs was validated: Leska-1-44 did not exhibit Pro129Gln, IP-Cot-0 did not exhibit
245 Gly182Ser and Grivo-1 did not exhibit Pro399Thr amino acid changes in *AtABCE1* (Supplementary Table
246 S4; Table 1). More interestingly, we verified Gly125Glu in IP-Cot-0 and Pro129Gln, Leu253Phe,
247 Ala441Thr and His561Leu in Grivo-1. Leu253Phe had not been annotated in any *A. thaliana* ecotype in the
248 1001 Genomes Project database (Table 1).

249 Surprisingly, we noticed some SNPs affecting highly conserved amino acid residues in AtABCE1.
250 These include arginine residues from R cluster of Hinge domains (Arg323Cys and Arg572Leu of IP-Moz-
251 0 and Toufl-1, respectively), and Arg86Gln of IP- Ezc-2 ecotype that locates to the Y-loop I (Figure 7 A;
252 Table 1). According to the 1001 Genomes Project database the latter SNP is present in 19 *A. thaliana*
253 ecotypes (Supplementary table S4).

254 Although, the length of AtABCE proteins in *A. thaliana* ecotypes is very conserved, in a single
255 ecotype, namely Kly-4, we found a SNP in *AtABCE1* causing premature stop codon that makes the protein
256 14 amino acid residues shorter. Despite this deletion, the cluster of arginine residues remains intact in Hinge
257 II subdomain (Supplementary Figure S5).

258

259 **Discussion**

260 The availability of high-quality plant genome sequences is growing day by day, which creates a
261 completely new and underexploited repository. It has been recognized that the plant genome evolution has
262 been very complex, including polyploidy, periods of rapid speciation and extinction (Leebens-Mack et al.
263 2019). Interestingly, massive expansions of gene families took place before the origins of green plants, land
264 plants and vascular plants (Leebens-Mack et al. 2019). Whole genome duplications (WGDs) that have
265 occurred at least 244 times throughout the evolution of plants and ferns (Leebens-Mack et al. 2019) increase
266 ploidy of genomes and largely impact gene family size variation within different lineages. Apart from
267 autopolyploidy, which results from intraspecies WGD events, there are also allopolyploid species, which
268 originate from interspecies hybrids and render gene evolution tracking challenging.

269 **How many *ABCE* genes plants have and need?**

270 As was previously mentioned, in most animal and in yeast species the *ABCE* gene family is
271 represented by a single gene that encodes the vital ABCE1 protein. In plant kingdom, *ABCE* gene family
272 size across different lineages is more variable. Based on the data from the public databases and our analysis
273 we were able to reconfirm the same number of *ABCE* genes for a selection of plant species. For example

274 there is a single gene in *C. hirsuta* (Kougioumoutzi et al. 2013), in *C. reinhardtii* (Li et al. 2022), in *Citrus*
275 *sinesis* and in *Theobroma cacao* (Navarro-Quiles et al. 2022). Similarly to previous studies, we reverified
276 two genes in *Zea mays* (Pang et al. 2013), in tomato (Ofori et al. 2018), in rice, and in *Populus trichocarpa*
277 (Navarro-Quiles et al. 2022). The same was true for five *ABCE* genes from *Brassica rapa* (Navarro-Quiles
278 et al. 2022). Intriguingly, Zhang and colleagues found three *ABCE* genes in barley, whereas our study
279 identified only two sequences with all canonical subunits (604 and 611 amino acids long) (Zhang et al.
280 2020). Moreover, for *Capsella rubella* we identified four *ABCE* genes as opposed to two sequences analyzed
281 earlier (Navarro-Quiles et al. 2022). Taken together, we found that plant *ABCE* genes do not comprise a
282 single-copy gene family, but rather should be classified as a low-copy gene family.

283 In terms of evolutionary perspective, the duplicates of genes resulting from WGD are often subject
284 to relaxed selection, meaning rapid mutation resulting in loss of function (Qiao et al. 2019). In this study
285 we did not notice significant correlation between *ABCE* gene family size and WGD events occurred in a
286 lineage, probably due to the elimination of defunctionalized *ABCE* duplicates in many species during
287 evolution. For example, in *Glycine max* and *Actinidia chinensis* after five documented WGD events they
288 retained a single *ABCE2* gene. Interestingly, the overexpression of *ABCE1* in yeast causes growth inhibition
289 (Dong et al. 2004), meaning that the amount of *ABCE* present – and therefore probably also the number of
290 hypothetical redundant genes – is critical for the well-functioning of translation, a crucial process.

291 However, when higher expression of a particular gene is beneficial, its duplicate might be retained
292 in the genome. This could be the case for the two *ABCE* paralogues in maize that are located close to each
293 in our phylogenetic analysis (Figure 4) and share the same expression pattern profiles (Pang et al. 2013).
294 Alternatively, as a result of faster evolution, gene duplicates may obtain novel functions or specialized
295 expression patterns (Prince & Pickett 2002). In Arabidopsis, *AtABCE1* and *AtABCE2* exhibit partial
296 functional redundancy. In contrast to *AtABCE2*, which is ubiquitously expressed, *AtABCE1* is mostly
297 present in generative organs and at relatively low levels (Yu et al. 2023; Klepikova et al. 2016; Navarro-
298 Quiles et al. 2022). This could mean an ongoing process of pseudogenization or subfunctionalization, where
299 the paralogues acquire specific roles. There is a growing evidence regarding ribosomal heterogeneity and

300 the existence of specialized cell-type-specific ribosomes (Xue & Barna 2012; Barna et al. 2022), suggesting
301 that AtABCE1 is involved in the regulation of translation in generative tissues. Paralogous *ABCE* genes in
302 plants may serve to provide specificity in fine-tuning translation and controlling cellular translome (Gerst
303 2018).

304 Our initial observations based on a simple correlation analysis revealed a weak correlation between
305 ploidy level and *ABCE* gene number. In the future, the determinants of *ABCE* copy number can be further
306 elucidated by including more species from diverse lineages and using statistical modelling that takes
307 phylogenetic structuring of the data also into account. These models could also potentially include other
308 information from the species that was not used for the present study, such as whether the species is annual
309 or perennial, their preferred mode of reproduction, or what kind of environments do they grow in.

310 **In plants *ABCE* genes are prone to duplicate**

311 In this study we analyzed 152 *ABCE* sequences from 76 plant species. This included the most well
312 studied plant *ABCE* gene – AtABCE2, which is thought to preserve the ancestral functions of *ABCE*
313 proteins (Navarro-Quiles et al. 2022). Phylogenetic tree of full-length *ABCE* protein sequences confirmed
314 previously reported clustering into *ABCE2* and *ABCE1* groups for *Brassicaceae* (Navarro-Quiles et al.
315 2022) but was unable to resolve the relationship between *ABCEs* from different families. The lack of
316 phylogenetic signal can at least partially be explained by the strong conservation of plant *ABCE* proteins,
317 each sharing at least 78% of sequence identity with AtABCE2 (Supplementary Table S3). However, using
318 the nucleotide sequences coding for *ABCE* proteins allowed to better illustrate the evolution and clustering
319 of plant *ABCE* genes. The results suggest that *Brassicaceae* and *Poaceae* families have undergone
320 independent lineage-specific splits of the ancestral *ABCE* gene. *Pooideae*, the largest *Poaceae* subfamily
321 that includes barley and wheat, appears to have had further duplication events and its members have
322 additional *ABCE* genes. In addition to *Brassicaceae* and *Poaceae*, many other plant taxa have also gained
323 *ABCE* gene copies, most likely as a result of more recent duplications. We can therefore postulate that in
324 contrast to species which possess a single *ABCE* gene and are sensitive to copy number changes (Dong et
325 al. 2004), plants have evolved to benefit from higher numbers of this essential translational factor. Gene

326 copies may arise from different events including WGD, tandem- and transposon-related duplications, but
327 the precise source of *ABCE* subfamily expansion in plants remains to be investigated.

328 **Natural variation of *A. thaliana* ABCEs**

329 Usually, essential genes are subject to strong evolutionary pressure and thus, non-synonymous
330 SNPs in conserved regions of gene sequences are rare (Pang et al. 2016; Castle 2011). In *AtABCE1* we
331 found three SNPs that could potentially impact the protein's function (Table1; Figure 7A). SNPs causing
332 the substitutions Arg323Cys (in IP-Moz-0) and Arg572Leu (in Toufl-1) located at Hinge domain I and II
333 could be of importance, since these domains are essential for NBD-twin cassette assembly in the case of
334 *ABCE1* in other organisms (Karcher et al. 2005). In addition, *AtABCE1* of IP-Ezc-2 ecotype contains an
335 amino acid substitution at position Arg86Gln, which is exceptionally conserved across archaea and
336 eukaryotes and locates to Y-loop I. In the context of Y-loop with consensus sequence **HRYGVNAF**, the
337 arginine residue has been shown to mediate interaction between FeS cluster domain and NBD1 in the sole
338 *ABCE1* gene of *Pyrococcus abyssi* (Karcher et al. 2008).

339 The His561Leu amino acid change was reported to be present in 997 out of 1135 *A. thaliana*
340 ecotypes (Supplementary Table S4), which suggest that histidine at this position of *AtABCE1* might be
341 characteristic only to a small subset of ecotypes including Col-0. Thus, it seems that leucine is the most
342 conserved residue at position 561 in *AtABCE1* among *Arabidopsis* ecotypes.

343 As expected, in *AtABCE2* gene, known to be essential for the viability of an organism (Navarro-Quiles et
344 al. 2022; Yu et al. 2023) only four non-synonymous SNPs residing in non-conserved regions were found
345 among 1135 *A. thaliana* ecotypes (Supplementary Table S4). Importantly, the *AtABCE2* gene seems to be
346 hard to mutate, since up to now there is no T-DNA homozygous line available and only one viable,
347 hypomorphic allele has been recently isolated after ethyl methanesulfonate mutagenesis (Navarro-Quiles et
348 al., 2022). Interestingly, the only non-synonymous SNP present in more than one ecotype in the case of
349 *AtABCE2* is leading to Gly44Ser substitution in FeS domain. According to the 1001 Genomes Project

350 database this mutation is present in 54 ecotypes, three of them were confirmed in the current study (Table
351 1; Figure 7; Supplementary Table S4).

352 Taken together, this study has shown the surprisingly high number of *ABCE* genes among the plant
353 kingdom. We hypothesize that plants have developed a number of specialized ABCEs with more specific
354 functions compared to species carrying a single copy of *ABCE* gene such as humans, fruit fly or yeast.

355

356 **Methods**

357 **Phylogenetic diagram of studied plants**

358 The phylogenetic diagram of the studied plants species together with the bar chart of *ABCE* gene
359 number was created based on NCBI taxonomy with phyloT and visualized with iTOL (Letunic & Bork
360 2007, 2019; phylot.biobyte.de).

361 **Genome and proteome data acquisition**

362 *ABCE* sequence data for 55 species was downloaded from the online resource Phytozome portal
363 <https://phytozome.jgi.doe.gov/> (Goodstein et al. 2012). *ABCE* sequence data for additional 18 species was
364 downloaded from Ensembl Plants (Howe et al. 2020). The genome data for *C. hirsuta* was accessed at
365 <http://bioinfo.mpipz.mpg.de/blast/> (Gan et al. 2016). Genome data for *N. tabacum* and *N. benthamiana* was
366 downloaded from Sol Genomics Network <http://solgenomics.net> (Edwards et al. 2017; Kourelis et al. 2019).
367 We downloaded genomic, CDS and translated amino acid sequences for each plant *ABCE* gene used in the
368 study.

369 The length of amino acid sequences was calculated with SeqinR package (version 3.6.1) in R 4.0.2
370 (Charif & Lobry 2007). In order to calculate their similarities to *AtABCE2*, all 152 sequences were aligned
371 using the online interface of MUSCLE with default Pearson/FASTA parameters provided by the European
372 Bioinformatics Institute (EBI) (Madeira et al. 2019). Thereafter the percent identity scores were calculated
373 with MUSCLE algorithm for aligned sequences in R 4.0.2 package Bio3D version 2.4-1 (Grant et al. 2021;
374 Edgar 2004).

375 Next, sequences aligned to AtABCE2 were inspected for the general protein structure, that is the
376 presence and correct order of the domains, including FeS cluster domain, NBD1, NBD2 and bipartite Hinge
377 domain (Supplementary Figure S6). Sequences lacking critical motifs within these domains (Karcher et al.
378 2005; Barthelme et al. 2007; Nürenberg & Tampé 2013; Nürenberg-Goloub et al. 2020) were filtered out
379 from the analysis.

380 **Evolutionary analysis by Maximum Likelihood method**

381 All amino acid sequences were analyzed with the MEGA software package (versions 10.2.2 and
382 11.0.13) (Kumar et al. 2018) as described below. Sequences were aligned with default parameters of the
383 MUSCLE algorithm. Phylogenetic relationships were inferred using the Maximum Likelihood method and
384 JTT matrix-based model (Jones et al. 1992), selected for each data set based on the lowest BIC scores
385 (Bayesian Information Criterion). A discrete gamma distribution was used to model evolutionary rate
386 differences among sites. Bootstrap analysis was performed with 500 replicates. The trees with the highest
387 log likelihood were published for each analysis.

388 CDS sequences were aligned with the default parameters of MAFFT version 7.4.9.0 (Katoh &
389 Standley 2013). Sites in the CDS alignment that contained gaps for more than 10% of the sequences were
390 removed with trimAl version 1.4.rev22 (Capella-Gutiérrez et al. 2009), resulting in 1,810 retained
391 positions. RAxML version 8.2.12 (Stamatakis 2014) was used to create a maximum likelihood phylogeny
392 with the GTR model of nucleotide substitution, gamma model of rate heterogeneity and 500 bootstrap
393 replicates.

394 **Data acquisition for 1135 Arabidopsis ecotypes**

395 Data (SNPs and indels) available for 1135 *A. thaliana* strains was downloaded from the 1001
396 Genomes Project depository (Weigel & Mott 2009).

397 **Reconfirming the haplotypes of Arabidopsis ecotypes**

398 Seeds of the selected 21 Arabidopsis ecotypes were acquired from the Nottingham Arabidopsis
399 Stock Centre (NASC). Both *AtABCE1* and *AtABCE2* full coding sequences were PCR-amplified and

400 sequenced by Sanger sequencing for ecotypes Can-0, Ei-2, IP-Car-1, Kia1 and Pra-6. For the other 15
401 ecotypes only *AtABCE1* full coding sequences was sequenced. Primer pairs used for the PCRs are shown in
402 the Supplementary Table S5. For all the PCR reactions touchdown PCR method with the following
403 conditions was used: 95 °C for 15 minutes; 13 cycles of at 95 °C for 15 seconds, at the gradually decreasing
404 temperature from 60 °C to 54 °C (the temperature drops by 0.5 °C per cycle) for 30 seconds, at 72°C for 70
405 seconds; 15 cycles of 95°C 15 seconds, 54°C 30 seconds, 72°C 70 seconds and the final extension at 72 °C
406 for 10 minutes. Amplified DNA fragments were purified from the agarose gel using GeneJET Gel Extraction
407 Kit (Thermo Scientific) according to the manufacturer's instructions. Thereafter the purified DNA
408 fragments were Sanger sequenced and aligned respectively to *AtABCE1* or *AtABCE2*. The final results were
409 based on the sequencing of at least two plants for each ecotype. Columbia (Col-0) ecotype was used as a
410 reference.

411 **Generating haplotype map with PopART**

412 For the haplotype analysis, first an alignment file with CDS sequences was created in Nexus format.
413 Thereafter the multiple sequence alignment was analyzed with PopART version 1.7 (Population Analysis
414 with Reticulate Trees) (Leigh & Bryant 2015). The network was constructed with Median Joining Network
415 algorithm (epsilon=0).

416

417 **Figure and table texts**

418 **Fig. 1. Phylogenetic diagram of 152 *ABCE* genes in plants.** The data was compiled from 76 plant species.
419 Whole genome duplications (WGDs) and triplications (WGT) are marked as grey and black stars,
420 respectively.

421 **Fig. 2. *ABCE* copy number in plants.** (A) *ABCE* gene copy number among the studied 76 plant species.
422 (B) The correlation between *ABCE* gene copy number and species ploidy level. (C) The correlation between
423 *ABCE* gene copy number and the number of WGDs of a species.

424 **Fig. 3. Amino acid sequences of plant *ABCE*s reveal high level of conservation.** (A) Linear protein
425 model of At*ABCE2*. Grey regions depict highly conserved motifs within At*ABCE2*. FeS – iron-sulphur
426 cluster domain, NBD1 – nucleotide-binding domain 1, NBD2 – nucleotide-binding domain 2. (B) Histogram
427 of protein sequence lengths of the studied 152 plant *ABCE*s. (C) Histogram of amino acid sequence
428 identities of the studied 152 plant *ABCE*s, based on MUSCLE alignment. (D) The correlation between
429 amino acid sequence identity and protein sequence length of the studied 152 plant *ABCE*s.

430 **Fig. 4. Cladogram of the 152 plant *ABCE* full-length amino acid sequences.** There was a total of 777
431 positions in the final dataset. The tree was constructed using the Maximum Likelihood method and JTT+G
432 model. Color coding of the selected proteins refers to the affiliation to the bigger plant phyla or families.
433 Bootstrap values over 75% are depicted on the figure. The tree is rooted on *Chlorophyta* phylum.

434 **Fig. 5. Cladogram of the selected 83 plant *ABCE* amino acid sequences from the *Brassicaceae* family
435 (32), *Poaceae* family (48) and *A. trichopoda* (2) together with *C. reinhardtii* (1) as the root of the tree.**
436 There was a total of 738 positions in the final dataset. The tree was constructed using the Maximum
437 Likelihood method and JTT+G model. Bootstrap values over 75% are depicted on the figure.

438 **Fig. 6. Cladogram of the 152 plant *ABCE* full-length CDS sequences.** There was a total of 1810 positions
439 in the final dataset. The tree was constructed using the Maximum Likelihood method and JTT+G model.
440 Color coding of the selected proteins refers to the affiliation to the bigger plant phyla or families. Bootstrap
441 values over 75% are depicted on the figure.

442 **Fig. 7. Analysis of non-synonymous SNPs in *AtABCE1* and *AtABCE2*.** (A) Linear protein model of
443 *AtABCE1*. Asterisks depict amino acid substitutions due to SNPs verified in different ecotypes. (B)
444 Haplotype map of *AtABCE1* detected among 22 *Arabidopsis* ecotypes. Branch length represents the number
445 of mutations between sequences. For pairs of haplotypes whose distances on the tree are longer than the
446 distances between the sequences, edges are added to shorten the distance. (C) Linear protein model of
447 *AtABCE2*. Asterisks depict amino acid substitutions due to SNPs verified in different ecotypes. (D)
448 Haplotype map of *AtABCE2* detected among six *Arabidopsis* ecotypes. Branch length represents the
449 number of mutations between sequences. For pairs of haplotypes whose distances on the tree are longer than
450 the distances between the sequences, edges are added to shorten the distance.

451 **Table 1. Non-synonymous SNPs found in *AtABCE1* and *AtABCE2* among 21 *A. thaliana* ecotypes.**

452 All SNPs were verified by Sanger sequencing and whole-genome sequencing published in the 1001
453 Genomes project (Weigel & Mott 2009; Cao et al. 2011). SNP locations were numbered according to the
454 position in the cDNA sequence starting from ATG. Change in amino acid sequence corresponding to the
455 SNP is presented. Orange color depicts SNPs that are not present in 1001 Genomes Project data but verified
456 by Sanger sequencing within this study. Green color shows SNPs positioned in conserved arginine residues.
457

458 **Supplementary Material**

459 **Supplementary Figure S1. Maximum likelihood phylogenetic trees supporting the use of *Chlorophyta***
460 **phylum as the outgroup for ABCE phylogenetic studies.** (A) Unrooted tree of 152 ABCE amino acid
461 sequences. Representatives of *Chlorophyta* formed a separate cluster with high bootstrap support. (B) Tree
462 with ABCE amino acid sequences from 15 selected plant species rooted on HsABCE1.

463 **Supplementary Figure S2. Cladogram of FeS domain of the 152 plant ABCEs.** There was a total of 113
464 positions in the final dataset. The tree was constructed using the Maximum Likelihood method and JTT+G
465 model. Color coding of the selected proteins refers to the affiliation to the bigger plant phyla or families.

466 **Supplementary Figure S3. Cladogram of NBD1 domain of the 152 plant ABCEs.** There was a total of
467 249 positions in the final dataset. The tree was constructed using the Maximum Likelihood method and

468 JTT+G model. Color coding of the selected proteins refers to the affiliation to the bigger plant phyla or
469 families.

470 **Supplementary Figure S4. Cladogram of NBD2 domain of the 152 plant ABCEs.** There was a total of
471 293 positions in the final dataset. The tree was constructed using the Maximum Likelihood method and
472 JTT+G model. Color coding of the selected proteins refers to the affiliation to the bigger plant phyla or
473 families.

474 **Supplementary Figure S5. Images of 22 *Arabidopsis* ecotypes.** White scale bar depicts 1 cm on the
475 images.

476 **Supplementary Figure S6. Alignment of human HsABCE1 and *Arabidopsis thaliana* AtABCE2**
477 **together with respective domains and conserved regions.**

478 **Supplementary Table S1. List of the 76 plant species used within the *ABCE* phylogenetic analysis.**
479 Number of plant *ABCE* genes identified per species, database used, genome assembly version and genome
480 ploidy level are depicted.

481 **Supplementary Table S2. Whole-genome duplications (WGDs) detected in the plant species analyzed**
482 **in the study.** Data is based on the results of One Thousand Plant Transcriptomes Initiative published in
483 2019.

484 **Supplementary Table S3. List of the 152 *ABCE* genes identified from 76 plant species together with**
485 **protein length and amino acid sequence similarity to AtABCE2.**

486 **Supplementary Table S4. Non-synonymous SNPs found in AtABCE1 and AtABCE2.**

487 **Supplementary Table S5. Primers used within this study.**

488 **Supplementary File S1. A Maximum Likelihood phylogenetic tree based on 152 plant *ABCE* full-**
489 **length amino acid sequences.** This data was used to create Figure 4 and is in Newick file format.

490 **Supplementary File S2. . A Maximum Likelihood phylogenetic tree based on selected 83 plant *ABCE***
491 **full-length amino acid sequences from the *Brassicaceae* family (32), *Poaceae* family (48) and *A.***
492 ***trichopoda* (2) together with *C. reinhardtii* (1) as the root of the tree.** This data was used to create Figure
493 5 and is in Newick file format.

494 **Supplementary File S3. A Maximum Likelihood phylogenetic tree based on 152 plant ABCE full-**
495 **length CDS sequences.** This data was used to create Figure 6 and is in Newick file format.

496

497 **Acknowledgements**

498 This work was supported by Postdoctoral grant SS458 to L. J. from Tallinn University of Technology. J.S.

499 was funded by a Natural Sciences and Engineering Research Council of Canada Discovery Grant to Colin

500 Garroway. The research was conducted using the equipment purchased within the framework of the Project

501 “Plant Biology Infrastructure – TAIM” funded by the EU Regional Development Fund (2014-2020.4.01.20-

502 0282).

503

504

505 **References**

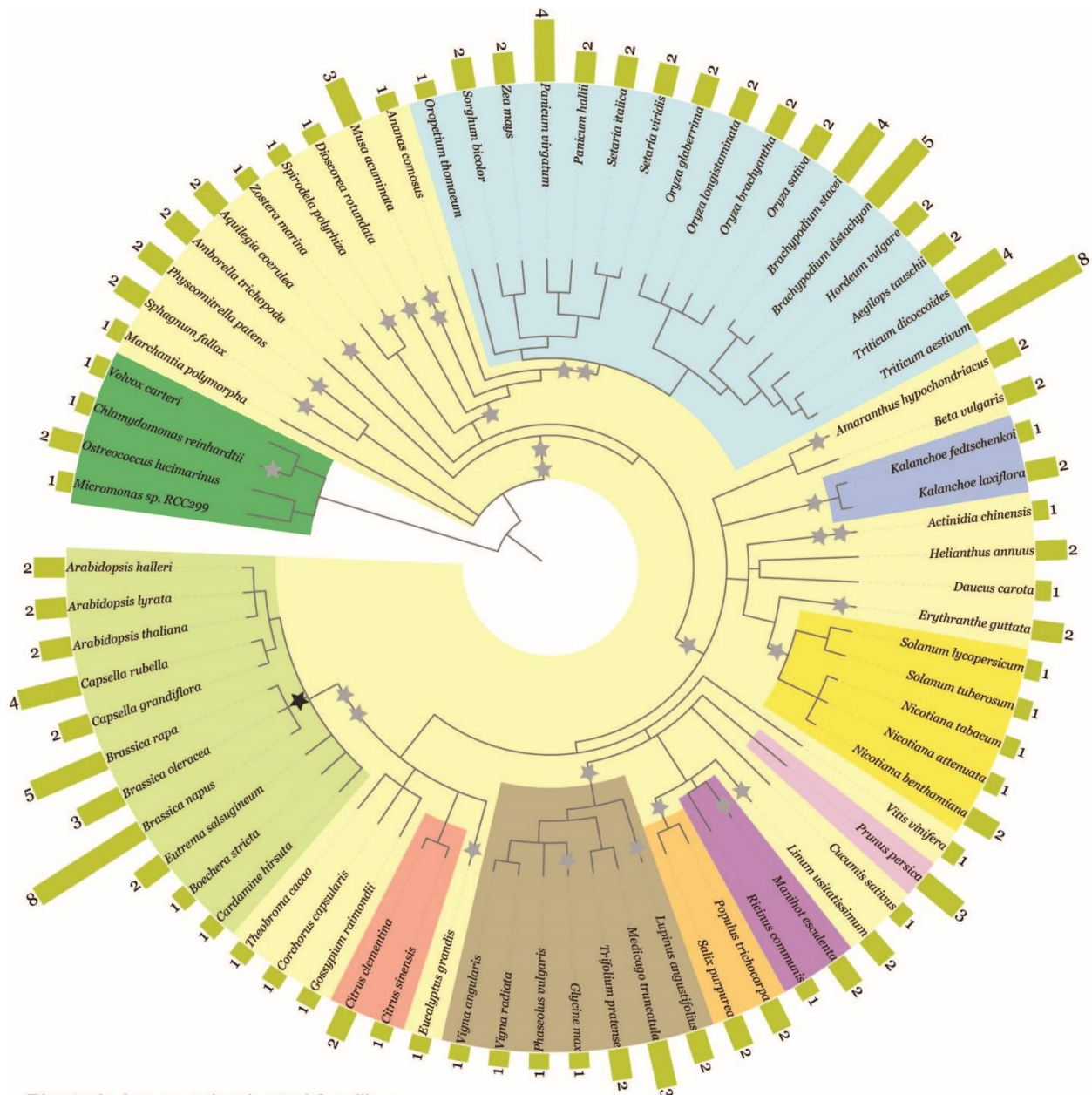
- 506 Andersen DS, Leever SJ. 2007. The Essential Drosophila ATP-binding Cassette Domain Protein, Pixie,
507 Binds the 40 S Ribosome in an ATP-dependent Manner and Is Required for Translation Initiation. *J. Biol.*
508 *Chem.* 282:14752–14760. doi: 10.1074/jbc.M701361200.
- 509 Andolfo G et al. 2015. Genetic variability and evolutionary diversification of membrane ABC transporters
510 in plants. *BMC Plant Biol.* 15:51. doi: 10.1186/s12870-014-0323-2.
- 511 Barna M et al. 2022. The promises and pitfalls of specialized ribosomes. *Mol. Cell.* 82:2179–2184. doi:
512 10.1016/j.molcel.2022.05.035.
- 513 Barthelme D et al. 2011. Ribosome recycling depends on a mechanistic link between the FeS cluster
514 domain and a conformational switch of the twin-ATPase ABCE1. *Proc. Natl. Acad. Sci. U. S. A.*
515 108:3228–3233. doi: 10.1073/pnas.1015953108.
- 516 Barthelme D et al. 2007. Structural organization of essential iron-sulfur clusters in the evolutionarily
517 highly conserved ATP-binding cassette protein ABCE1. *J. Biol. Chem.* 282:14598–14607. doi:
518 10.1074/jbc.M700825200.
- 519 Braz ASK, Finnegan J, Waterhouse P, Margis R. 2004. A plant orthologue of RNase L inhibitor (RLI) is
520 induced in plants showing RNA interference. *J. Mol. Evol.* 59:20–30. doi: 10.1007/s00239-004-2600-4.
- 521 Capella-Gutiérrez S, Silla-Martínez JM, Gabaldón T. 2009. trimAl: a tool for automated alignment
522 trimming in large-scale phylogenetic analyses. *Bioinformatics.* 25:1972–1973. doi:
523 10.1093/bioinformatics/btp348.
- 524 Castle JC. 2011. SNPs occur in regions with less genomic sequence conservation. *PloS One.* 6:e20660.
525 doi: 10.1371/journal.pone.0020660.
- 526 Charif D, Lobry JR. 2007. SeqinR 1.0-2: A Contributed Package to the R Project for Statistical
527 Computing Devoted to Biological Sequences Retrieval and Analysis. In: *Structural Approaches to*
528 *Sequence Evolution: Molecules, Networks, Populations.* Bastolla, U, Porto, M, Roman, HE, &
529 Vendruscolo, M, editors. Biological and Medical Physics, Biomedical Engineering Springer: Berlin,
530 Heidelberg pp. 207–232. doi: 10.1007/978-3-540-35306-5_10.
- 531 Dermauw W, Van Leeuwen T. 2014. The ABC gene family in arthropods: comparative genomics and role
532 in insecticide transport and resistance. *Insect Biochem. Mol. Biol.* 45:89–110. doi:
533 10.1016/j.ibmb.2013.11.001.
- 534 Dong J et al. 2004. The essential ATP-binding cassette protein RLI1 functions in translation by promoting
535 preinitiation complex assembly. *J. Biol. Chem.* 279:42157–42168. doi: 10.1074/jbc.M404502200.
- 536 Du X et al. 2003. cDNA Cloning and Expression Analysis of the Rice (*Oryza sativa* L.) RNase L
537 Inhibitor. *DNA Seq.* 14:295–301. doi: 10.1080/1085566031000141162.
- 538 Edgar RC. 2004. MUSCLE: multiple sequence alignment with high accuracy and high throughput.
539 *Nucleic Acids Res.* 32:1792–1797. doi: 10.1093/nar/gkh340.

- 540 Edwards KD et al. 2017. A reference genome for *Nicotiana tabacum* enables map-based cloning of
541 homeologous loci implicated in nitrogen utilization efficiency. *BMC Genomics*. 18:448. doi:
542 10.1186/s12864-017-3791-6.
- 543 Gan X et al. 2016. The *Cardamine hirsuta* genome offers insight into the evolution of morphological
544 diversity. *Nat. Plants*. 2:1–7. doi: 10.1038/nplants.2016.167.
- 545 Garcia O, Bouige P, Forestier C, Dassa E. 2004. Inventory and comparative analysis of rice and
546 *Arabidopsis* ATP-binding cassette (ABC) systems. *J. Mol. Biol.* 343:249–265. doi:
547 10.1016/j.jmb.2004.07.093.
- 548 Gerst JE. 2018. Pimp My Ribosome: Ribosomal Protein Paralogs Specify Translational Control. *Trends*
549 *Genet.* 34:832–845. doi: 10.1016/j.tig.2018.08.004.
- 550 Goodstein DM et al. 2012. Phytozome: a comparative platform for green plant genomics. *Nucleic Acids*
551 *Res.* 40:D1178–D1186. doi: 10.1093/nar/gkr944.
- 552 Graille M, Séraphin B. 2012. Surveillance pathways rescuing eukaryotic ribosomes lost in translation.
553 *Nat. Rev. Mol. Cell Biol.* 13:727–735. doi: 10.1038/nrm3457.
- 554 Grant BJ, Skjaerven L, Yao X-Q. 2021. The Bio3D packages for structural bioinformatics. *Protein Sci.*
555 *Publ. Protein Soc.* 30:20–30. doi: 10.1002/pro.3923.
- 556 Howe KL et al. 2020. Ensembl Genomes 2020—enabling non-vertebrate genomic research. *Nucleic Acids*
557 *Res.* 48:D689–D695. doi: 10.1093/nar/gkz890.
- 558 Jones DT, Taylor WR, Thornton JM. 1992. The rapid generation of mutation data matrices from protein
559 sequences. *Bioinformatics*. 8:275–282. doi: 10.1093/bioinformatics/8.3.275.
- 560 Kärblane K et al. 2015. ABCE1 is a highly conserved RNA silencing suppressor. *PLoS One*. 10:e0116702.
561 doi: 10.1371/journal.pone.0116702.
- 562 Karcher A, Büttner K, Märten B, Jansen R-P, Hopfner K-P. 2005. X-ray structure of RLI, an essential
563 twin cassette ABC ATPase involved in ribosome biogenesis and HIV capsid assembly. *Struct. Lond. Engl.*
564 1993. 13:649–659. doi: 10.1016/j.str.2005.02.008.
- 565 Karcher A, Schele A, Hopfner K-P. 2008. X-ray structure of the complete ABC enzyme ABCE1 from
566 *Pyrococcus abyssi*. *J. Biol. Chem.* 283:7962–7971. doi: 10.1074/jbc.M707347200.
- 567 Katoh K, Standley DM. 2013. MAFFT Multiple Sequence Alignment Software Version 7: Improvements
568 in Performance and Usability. *Mol. Biol. Evol.* 30:772–780. doi: 10.1093/molbev/mst010.
- 569 Kispal G et al. 2005. Biogenesis of cytosolic ribosomes requires the essential iron–sulphur protein Rli1p
570 and mitochondria. *EMBO J.* 24:589–598. doi: 10.1038/sj.emboj.7600541.
- 571 Klepikova AV, Kasianov AS, Gerasimov ES, Logacheva MD, Penin AA. 2016. A high resolution map of
572 the *Arabidopsis thaliana* developmental transcriptome based on RNA-seq profiling. *Plant J.* 88:1058–
573 1070. doi: 10.1111/tpj.13312.
- 574 Kougioumoutzi E et al. 2013. SIMPLE LEAF3 encodes a ribosome-associated protein required for leaflet
575 development in *Cardamine hirsuta*. *Plant J.* 73:533–545. doi: 10.1111/tpj.12072.

- 576 Kourelis J et al. 2019. A homology-guided, genome-based proteome for improved proteomics in the
577 allopolyploid *Nicotiana benthamiana*. *BMC Genomics*. 20:722. doi: 10.1186/s12864-019-6058-6.
- 578 Kumar S, Stecher G, Li M, Knyaz C, Tamura K. 2018. MEGA X: Molecular Evolutionary Genetics
579 Analysis across Computing Platforms. *Mol. Biol. Evol.* 35:1547–1549. doi: 10.1093/molbev/msy096.
- 580 Leebens-Mack JH et al. 2019. One thousand plant transcriptomes and the phylogenomics of green plants.
581 *Nature*. 574:679–685. doi: 10.1038/s41586-019-1693-2.
- 582 Leigh JW, Bryant D. 2015. popart: full-feature software for haplotype network construction. *Methods*
583 *Ecol. Evol.* 6:1110–1116. doi: <https://doi.org/10.1111/2041-210X.12410>.
- 584 Letunic I, Bork P. 2007. Interactive Tree Of Life (iTOL): an online tool for phylogenetic tree display and
585 annotation. *Bioinforma. Oxf. Engl.* 23:127–128. doi: 10.1093/bioinformatics/btl529.
- 586 Letunic I, Bork P. 2019. Interactive Tree Of Life (iTOL) v4: recent updates and new developments.
587 *Nucleic Acids Res.* 47:W256–W259. doi: 10.1093/nar/gkz239.
- 588 Li Xiangyu et al. 2022. Identification and Characterization of ATP-Binding Cassette Transporters in
589 *Chlamydomonas reinhardtii*. *Mar. Drugs*. 20:603. doi: 10.3390/md20100603.
- 590 Liu S, Li Q, Liu Z. 2013. Genome-wide identification, characterization and phylogenetic analysis of 50
591 catfish ATP-binding cassette (ABC) transporter genes. *PloS One*. 8:e63895. doi:
592 10.1371/journal.pone.0063895.
- 593 Lu H, Xu Y, Cui F. 2016. Phylogenetic analysis of the ATP-binding cassette transporter family in three
594 mosquito species. *Pestic. Biochem. Physiol.* 132:118–124. doi: 10.1016/j.pestbp.2015.11.006.
- 595 Madeira F et al. 2019. The EMBL-EBI search and sequence analysis tools APIs in 2019. *Nucleic Acids*
596 *Res.* 47:W636–W641. doi: 10.1093/nar/gkz268.
- 597 Maeda T et al. 2005. Cloning and characterization of a ribonuclease L inhibitor from the silkworm,
598 *Bombyx mori*. *DNA Seq.* 16:21–27. doi: 10.1080/10425170400028871.
- 599 Mancera-Martínez E, Brito Querido J, Valasek LS, Simonetti A, Hashem Y. 2017. ABCE1: A special
600 factor that orchestrates translation at the crossroad between recycling and initiation. *RNA Biol.* 14:1279–
601 1285. doi: 10.1080/15476286.2016.1269993.
- 602 Möttus J, Maiste S, Eek P, Truve E, Sarmiento C. 2021. Mutational analysis of *Arabidopsis thaliana*
603 ABCE2 identifies important motifs for its RNA silencing suppressor function. *Plant Biol.* 23:21–31. doi:
604 <https://doi.org/10.1111/plb.13193>.
- 605 Navarro-Quiles C et al. 2022. The *Arabidopsis* ATP-Binding Cassette E protein ABCE2 is a conserved
606 component of the translation machinery. *Front. Plant Sci.* 13.
607 <https://www.frontiersin.org/articles/10.3389/fpls.2022.1009895> (Accessed January 6, 2023).
- 608 Navarro-Quiles C, Mateo-Bonmatí E, Micol JL. 2018. ABCE Proteins: From Molecules to Development.
609 *Front. Plant Sci.* 9:1125. doi: 10.3389/fpls.2018.01125.
- 610 Nürenberg E, Tampé R. 2013. Tying up loose ends: ribosome recycling in eukaryotes and archaea. *Trends*
611 *Biochem. Sci.* 38:64–74. doi: 10.1016/j.tibs.2012.11.003.

- 612 Nürenberg-Goloub E et al. 2020. Molecular analysis of the ribosome recycling factor ABCE1 bound to the
613 30S post-splitting complex. *EMBO J.* n/a:e103788. doi: 10.15252/emj.2019103788.
- 614 Ofori PA et al. 2018. Tomato ATP-Binding Cassette Transporter SlABCB4 Is Involved in Auxin
615 Transport in the Developing Fruit. *Plants Basel Switz.* 7:65. doi: 10.3390/plants7030065.
- 616 Pang E, Wu X, Lin K. 2016. Different evolutionary patterns of SNPs between domains and unassigned
617 regions in human protein-coding sequences. *Mol. Genet. Genomics.* 291:1127–1136. doi:
618 10.1007/s00438-016-1170-7.
- 619 Pang K, Li Y, Liu M, Meng Z, Yu Y. 2013. Inventory and general analysis of the ATP-binding cassette
620 (ABC) gene superfamily in maize (*Zea mays* L.). *Gene.* 526:411–428. doi: 10.1016/j.gene.2013.05.051.
- 621 Petersen BO, Jørgensen B, Albrechtsen M. 2004. Isolation and RNA silencing of homologues of the
622 RNase L inhibitor in *Nicotiana* species. *Plant Sci.* 167:1283–1289. doi: 10.1016/j.plantsci.2004.06.030.
- 623 phylot.biobyte.de. phyloT : a phylogenetic tree generator. <https://phylot.biobyte.de/> (Accessed March 18,
624 2021).
- 625 Prince VE, Pickett FB. 2002. Splitting pairs: the diverging fates of duplicated genes. *Nat. Rev. Genet.*
626 3:827–837. doi: 10.1038/nrg928.
- 627 Qiao X et al. 2019. Gene duplication and evolution in recurring polyploidization–diploidization cycles in
628 plants. *Genome Biol.* 20:38. doi: 10.1186/s13059-019-1650-2.
- 629 Sarmiento C, Nigul L, Kazantseva J, Buschmann M, Truve E. 2006. AtRLI2 is an endogenous suppressor
630 of RNA silencing. *Plant Mol. Biol.* 61:153–163. doi: 10.1007/s11103-005-0001-8.
- 631 Stamatakis A. 2014. RAxML version 8: a tool for phylogenetic analysis and post-analysis of large
632 phylogenies. *Bioinformatics.* 30:1312–1313. doi: 10.1093/bioinformatics/btu033.
- 633 Strunk BS, Novak MN, Young CL, Karbstein K. 2012. Joining of 60S subunits and a translation-like
634 cycle in 40S ribosome maturation. *Cell.* 150:111–121. doi: 10.1016/j.cell.2012.04.044.
- 635 Toompuu M, Kärblane K, Pata P, Truve E, Sarmiento C. 2016. ABCE1 is essential for S phase
636 progression in human cells. *Cell Cycle Georget. Tex.* 15:1234–1247. doi:
637 10.1080/15384101.2016.1160972.
- 638 Verrier PJ et al. 2008. Plant ABC proteins--a unified nomenclature and updated inventory. *Trends Plant*
639 *Sci.* 13:151–159. doi: 10.1016/j.tplants.2008.02.001.
- 640 Wang X et al. 2011. The genome of the mesopolyploid crop species *Brassica rapa*. *Nat. Genet.* 43:1035–
641 1039. doi: 10.1038/ng.919.
- 642 Weigel D, Mott R. 2009. The 1001 Genomes Project for *Arabidopsis thaliana*. *Genome Biol.* 10:107. doi:
643 10.1186/gb-2009-10-5-107.
- 644 Xue S, Barna M. 2012. Specialized ribosomes: a new frontier in gene regulation and organismal biology.
645 *Nat. Rev. Mol. Cell Biol.* 13:355–369. doi: 10.1038/nrm3359.
- 646 Yarunin A et al. 2005. Functional link between ribosome formation and biogenesis of iron–sulfur proteins.
647 *EMBO J.* 24:580–588. doi: 10.1038/sj.emboj.7600540.

- 648 Yu S-X et al. 2023. RLI2 regulates Arabidopsis female gametophyte and embryo development by
649 facilitating the assembly of the translational machinery. *Cell Rep.* 42. doi: 10.1016/j.celrep.2023.112741.
- 650 Zhang Z et al. 2020. Genome-Wide Identification of Barley ABC Genes and Their Expression in
651 Response to Abiotic Stress Treatment. *Plants Basel Switz.* 9:1281. doi: 10.3390/plants9101281.
- 652 Zhao Z, Fang LL, Johnsen R, Baillie DL. 2004. ATP-binding cassette protein E is involved in gene
653 transcription and translation in *Caenorhabditis elegans*. *Biochem. Biophys. Res. Commun.* 323:104–111.
654 doi: 10.1016/j.bbrc.2004.08.068.
- 655 Zimmerman C et al. 2002. Identification of a host protein essential for assembly of immature HIV-1
656 capsids. *Nature.* 415:88–92. doi: 10.1038/415088a.
- 657

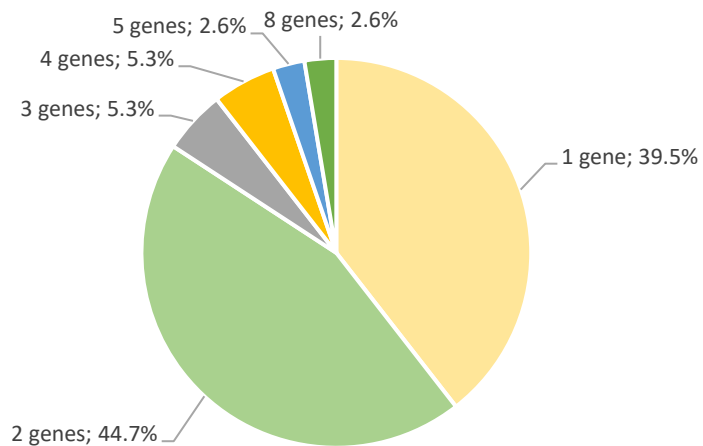


Plant phylums and selected families

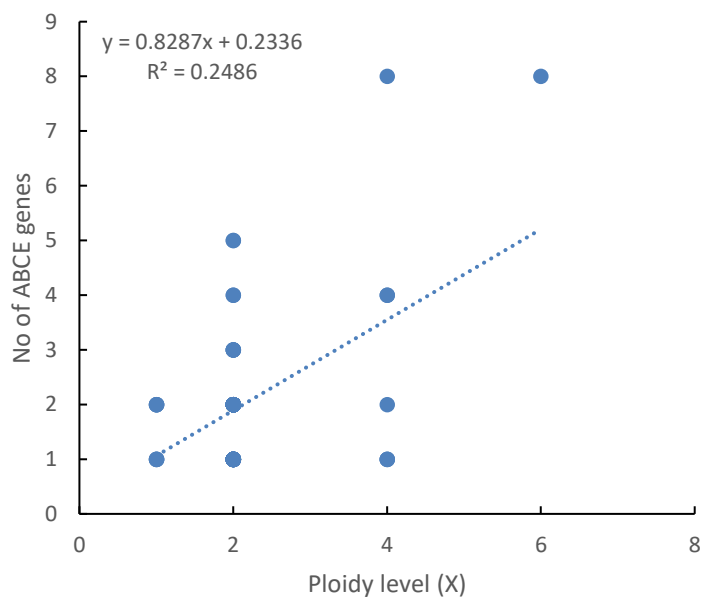
- | | |
|---|--|
| ■ Chlorophyta | ■ Euphorbiaceae |
| ■ Embryophyta | ■ Salicaceae |
| ■ Poaceae | ■ Fabaceae |
| ■ Crassulaceae | ■ Rutaceae |
| ■ Solanaceae | ■ Brassicaceae |
| ■ Rosaceae | ★ Whole genome duplication |
| | ★ Whole genome triplication |

Fig. 1.

(A)



(B)



(C)

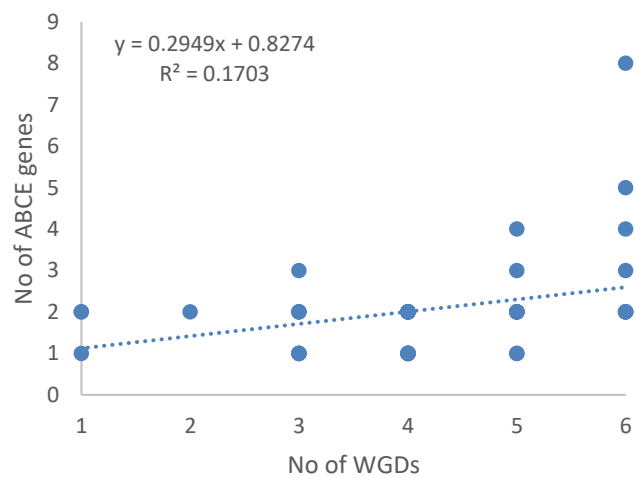


Fig. 2.

(A)

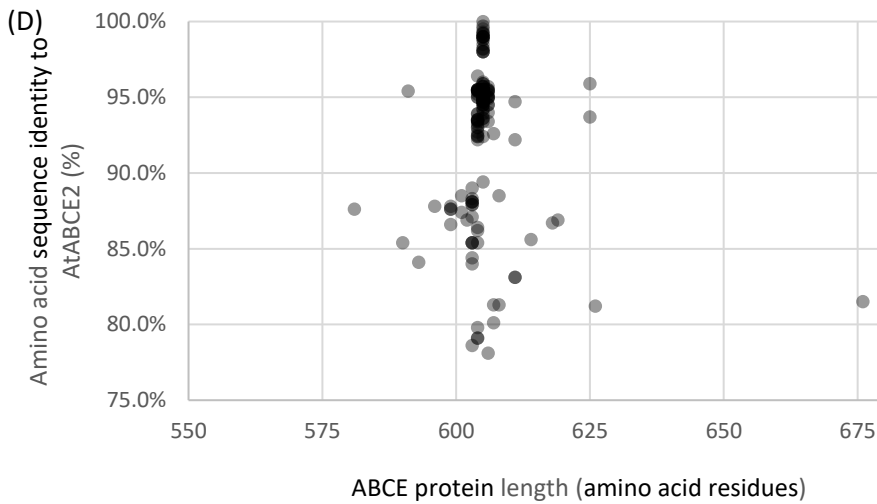
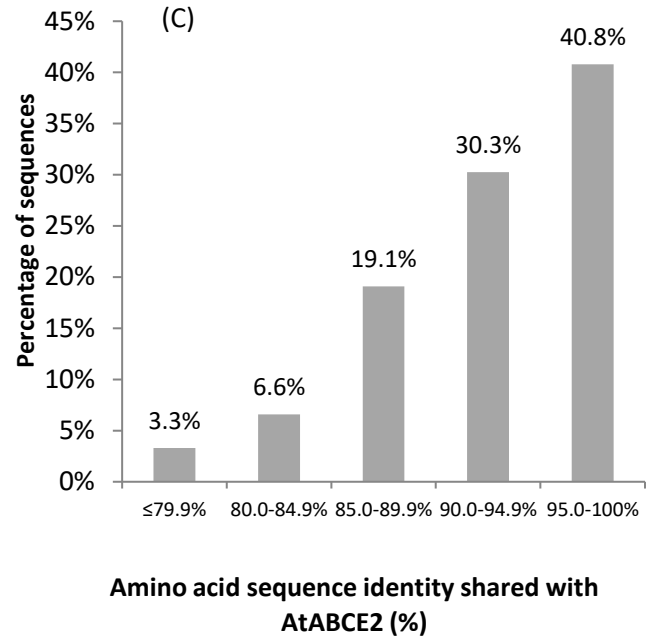
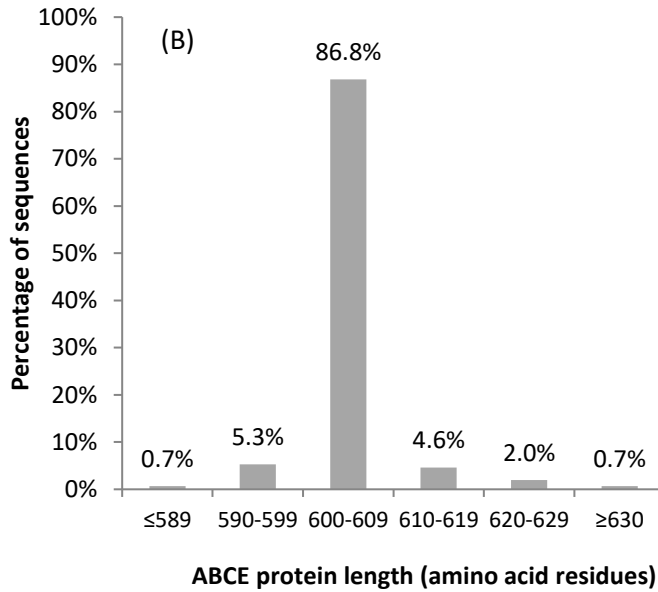
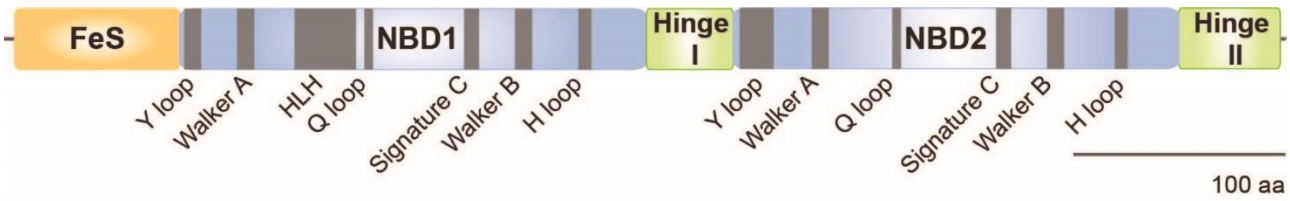


Fig. 3.

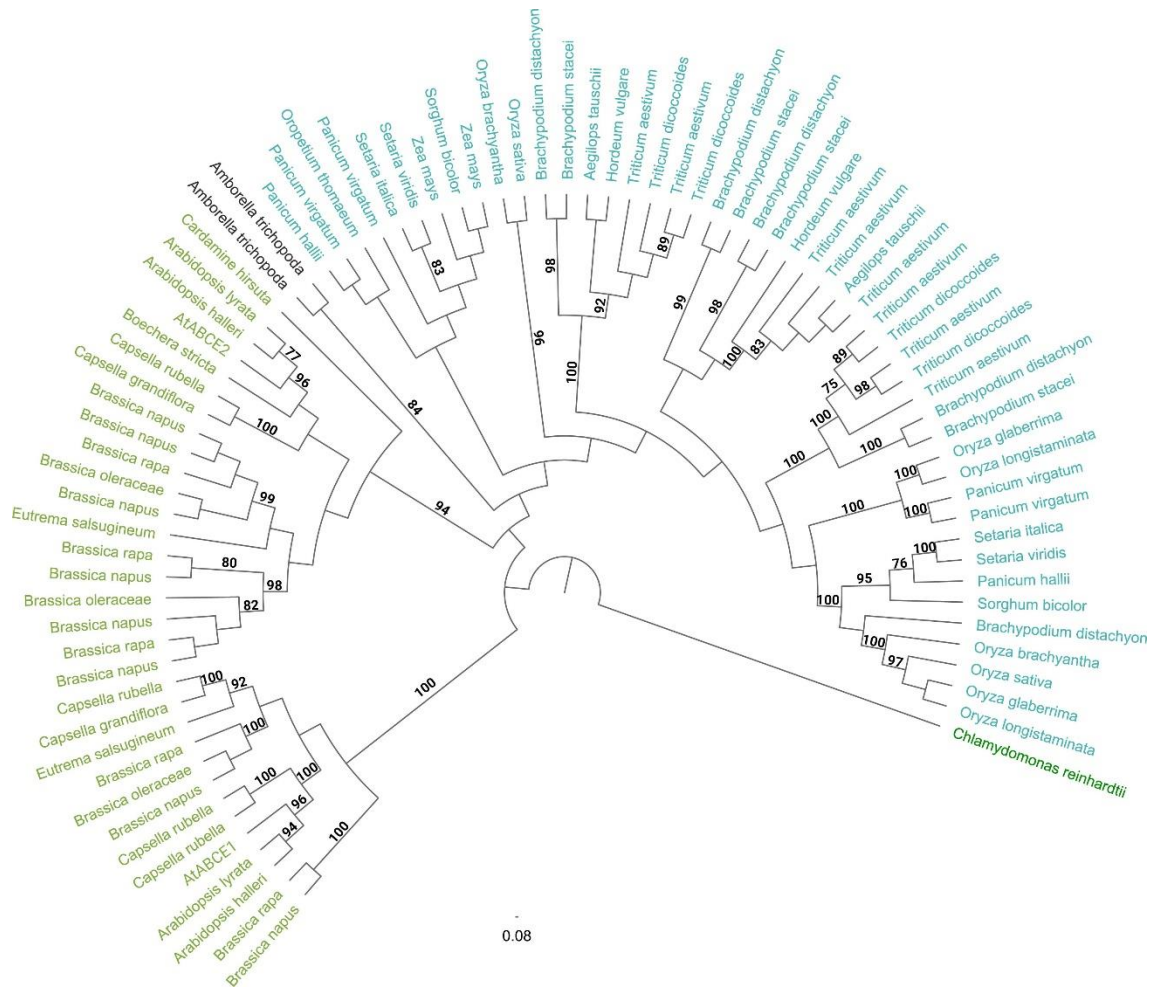


Fig. 5.

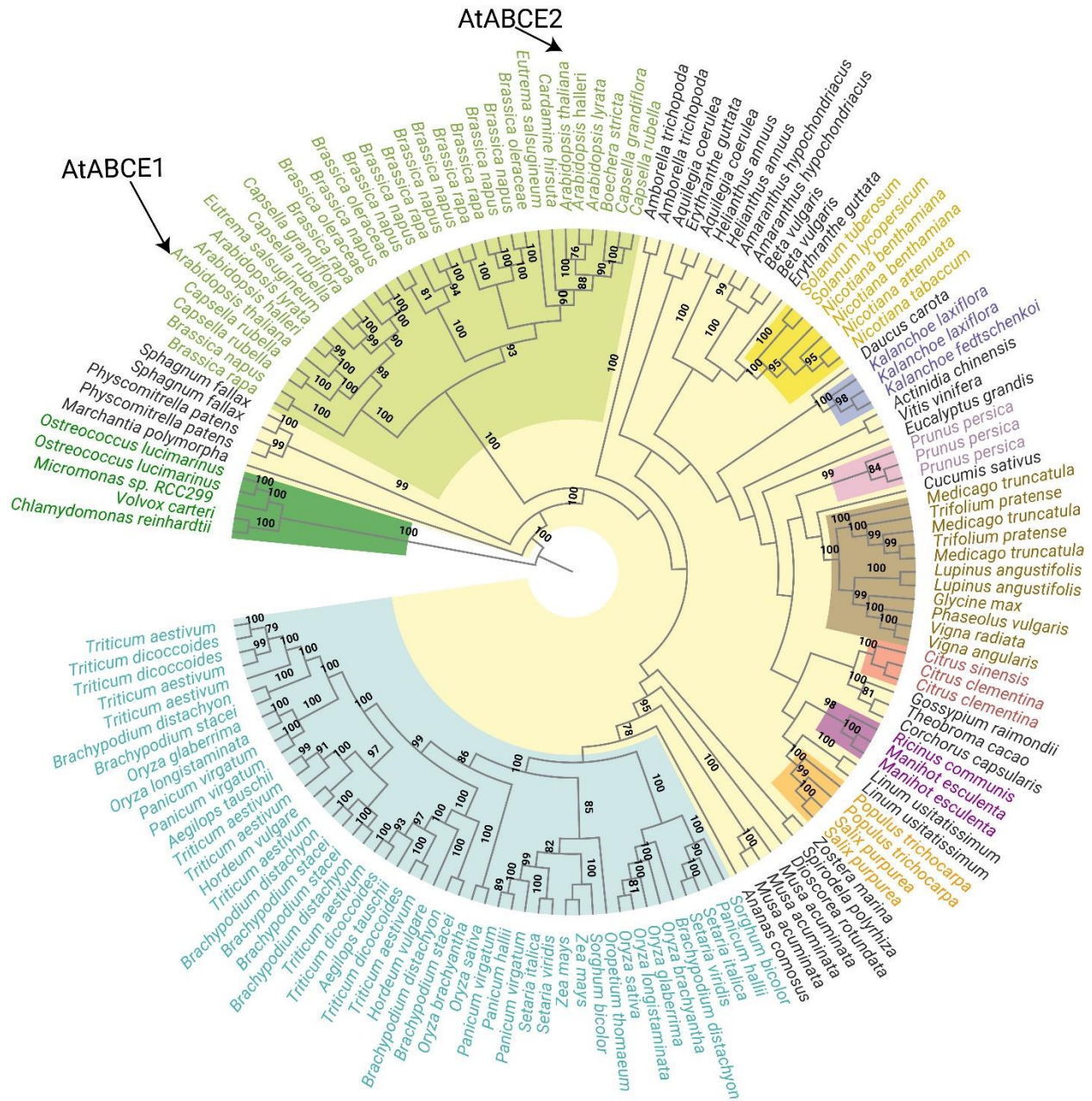


Fig. 6.

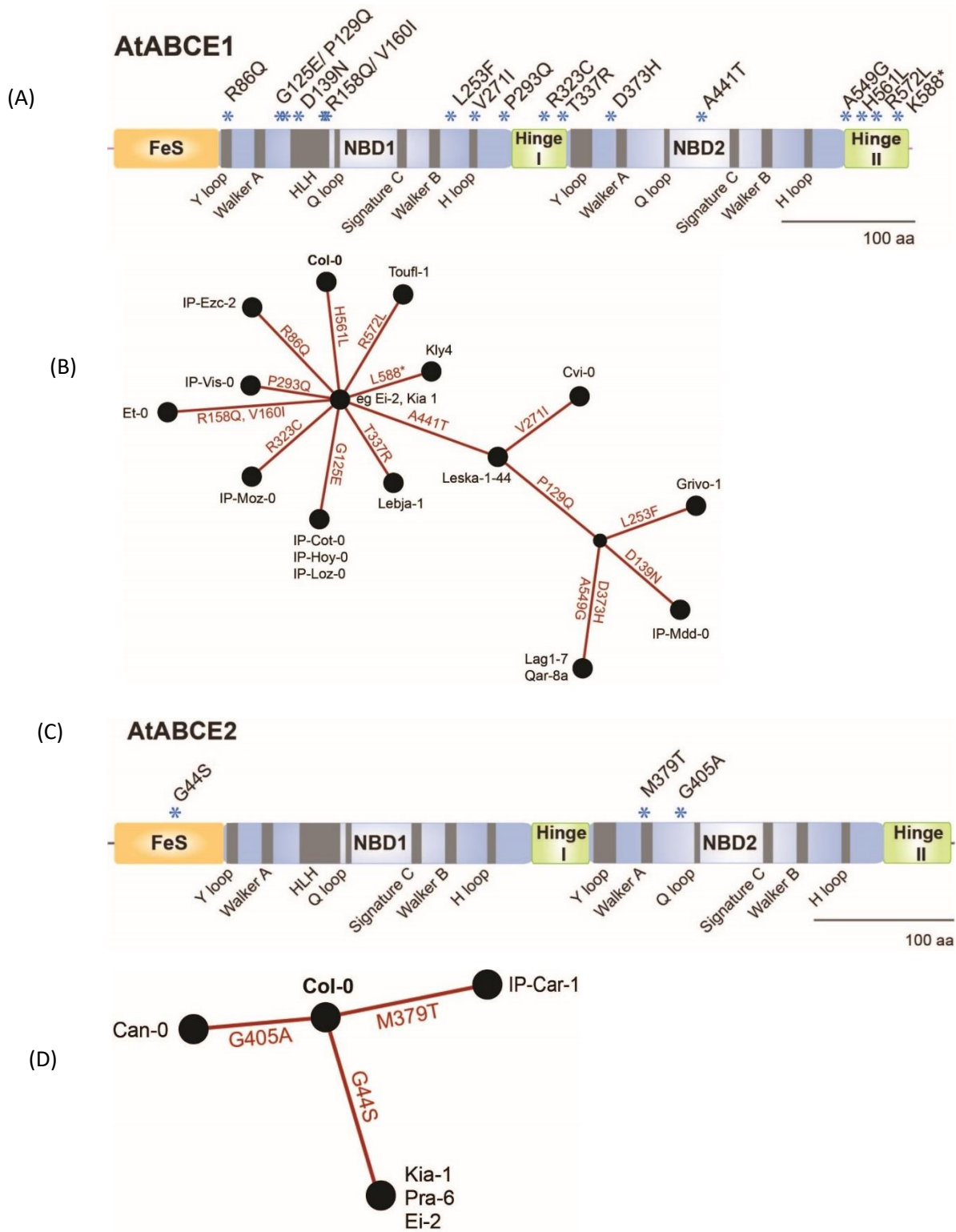


Fig. 7.

Table 1.

No	Ecotype	SNPs in <i>AtABCE1</i> cDNA	Amino acid change in <i>AtABCE1</i>	SNPs in <i>AtABCE2</i> cDNA	Amino acid change in <i>AtABCE2</i>	Origin
1	IP-Ezc-2	257G>A 1682A>T	Arg86Gln His561Leu	None	None	Spain
2	IP-Cot-0	374G>A 1682A>T	Gly125Glu His561Leu	None	None	Spain
3	IP-Hoy-0	374G>A 1682A>T	Gly125Glu His561Leu	None	None	Spain
4	IP-Loz-0	374G>A 1682A>T	Gly125Glu His561Leu	None	None	Spain
5	IP-Vis-0	878C>A 1682A>T	Pro293Gln His561Leu	None	None	Spain
6	IP-Moz-0	967C>T 1682A>T	Arg323Cys His561Leu	None	None	Spain
7	Lebja-1	1010C>G 1682A>T	Thr337Arg His561Leu	None	None	Russia
8	Leska-1-44	1321G>A 1682A>T	Ala441Thr His561Leu	None	None	Bulgaria
9	Toufl-1	1682A>T 1715G>T	His561Leu Arg572Leu	None	None	Morocco
10	Kly4	1682A>T 1762A>T	His561Leu Lys588STOP	None	None	Russia
11	Et-0	473G>A 478G>A 1682A>T	Arg158Gln Val160Ile His561Leu	None	None	France
12	Cvi-0	811G>A 1321G>A 1682A>T	Val271Ile Ala441Thr His561Leu	None	None	Cape Verde
13	IP-Mdd-0	386C>A 415G>A 1321G>A 1682A>T	Pro129Gln Asp139Asn Ala441Thr His561Leu	None	None	Spain
14	Grivo-1	386C>A 757C>T 1321G>A 1682A>T	Pro129Gln Leu253Phe Ala441Thr His561Leu	None	None	Bulgaria
15	Lag1-7	386C>A 1117G>C 1321G>A 1646C>G 1682A>T	Pro129Gln Asp373His Ala441Thr Ala549Gly His561Leu	None	None	Georgia
16	Qar-8a	386C>A 1117G>C 1321G>A 1646C>G 1682A>T	Pro129Gln Asp373His Ala441Thr Ala549Gly His561Leu	None	None	Lebanon
17	Ei-2	1682A>T	His561Leu	130G>A	Gly44Ser	Germany
18	Kia 1	1682A>T	His561Leu	130G>A	Gly44Ser	Sweden
19	Pra-6	1682A>T	His561Leu	130G>A	Gly44Ser	Spain
20	IP-Car-1	1682A>T	His561Leu	1136T>C	Met379Thr	Spain
21	Can-0	1682A>T	His561Leu	1214G>C	Gly405Ala	Spain